Published in "Sedimentary Geology 331: 148–161, 2016"
which should be cited to refer to this work.

Bryozoan beds in northern Italy as a shallow-water expression of environmental changes during the Oligocene isotope event 1

David Jaramillo-Vogel [a,*], Telm Bover-Arnal [b], André Strasser [a]

[a] Department of Geosciences, University of Fribourg, Chemin du Musée 6, 1700 Fribourg, Switzerland
[b] Departament de Geoquímica, Petrologia i Prospecció Geològica, Facultat de Geologia, Universitat de Barcelona, Martí i Franquès s/n, 08028 Barcelona, Spain

Shifts in carbonate-producing biotic communities in the geological record provide evidence of past environmental changes in the neritic realm. The shallow-marine Calcare di Nago Formation exposed in the San Valentino section (northern Italy) covers the Late Eocene and Earliest Oligocene. The succession is characterized by the occurrence of light-dependent biota such as coralline algae and larger benthic foraminifera. In the uppermost part of the section, however,\ the fossil association is dominated by bryozoans, which are filter-feeder organisms. This ca. 12 m thick interval locally contains up to 86% bryozoans, while coralline algae as well as larger benthic foraminifera are absent. Coralline algae and nummulitid foraminifera recover in the upper part of the bryozoan beds, whereas orthophragminids do not recover. The gradual disappearance of larger foraminifera and coralline algae within the bryozoan-dominated deposits is coeval with a pronounced positive shift in $\delta^{13}C$. Based on its biostratigraphic position, this positive shift is interpreted to be linked to the positive shift in $\delta^{13}C$ recognized in deep-sea records shortly above the Eocene–Oligocene boundary, which in turn is associated to the positive shift in $\delta^{18}O$ leading to the Oi-1 (Oligocene isotope event 1) cooling phase. Total phosphorus content increases in the bryozoan beds, suggesting enhanced nutrient supply to the neritic ecosystem. This phosphorous peak is coeval with the globally recognized increment in ocean productivity around the Oi-1 and $\delta^{13}C$ positive shift. Thus, disappearance of light-dependent biota and the dominance of bryozoans in the platform carbonates studied are interpreted to result not necessarily from a deepening of the depositional environment but from the combination of lower sea-surface temperatures and the deterioration of underwater light conditions on account of elevated turbidity in surface waters, resulting from enhanced primary productivity. As bryozoan beds occur in several Italian localities around the Eocene–Oligocene boundary, they are interpreted to represent the regional expression of neritic carbonate depositional systems to global environmental changes occurring at the dawn of an ice-house Earth.

1. Introduction

From the Middle Eocene to the Early Oligocene, the Earth experienced a pronounced cooling, leading to the initiation of the Antarctic glaciation and, consequently, to the beginning of the present ice-house world. The isotopic events characterizing the Eocene–Oligocene transition (EOT) are recorded as a two-stepped positive shift in both oxygen and carbon stable isotopes that lasted about 500 kyr (overview in Coxall and Pearson, 2007). The Oligocene isotope event 1 (Oi-1; Zachos et al., 1996; Katz et al., 2008; Miller et al., 2008, 2009), occurring at around 33.55 Ma, is characterized in deep-sea deposits by an up to 1‰ positive shift in $\delta^{18}O$. Despite advances made in recent years (Katz et al., 2008; Miller et al., 2008, 2009; Coxall and Wilson, 2011), little is known about the effect of the cooling associated to the Oi-1 in shallow-marine environments. On one hand, shallow-marine sedimentary records are incomplete in nature due to hiatuses and erosive processes. On the other hand, the correlation of shallow benthic biozones with stable isotope-, magneto-, and calcareous plankton stratigraphy in pelagic sections remains poorly constrained. Thus, the potential of environmentally sensitive shallow-marine deposits for interpreting this climate transition remains largely unexplored.

In the Cenozoic, light-dependent marine carbonate-producing organisms mainly correspond to zooxanthellate corals, symbiont-bearing larger foraminifera, red algae and green algae, while heterotrophic biota are dominated by bryozoans, molluscs, echinoderms and small benthic foraminifera. Based on biostratigraphic and chemostratigraphic data, Jaramillo-Vogel et al. (2013) correlated Eocene–Oligocene shallow-marine carbonate deposits belonging to the Calcare di Nago Formation from northern Italy with the shallow-water succession from Priabona (northern Italy) and deep-marine records of the Massignano section (central Italy), ODP Site 744 (southern Indian Ocean), and the Tanzania Drilling Project (TDP) Sites 12 and 17. This correlation highlights that the change from a shallow-marine phototrophic to a heterotrophic carbonate factory observed in several localities in northern Italy was related to the global cooling pulse occurring

* Corresponding author.
E-mail address: david.jaramillovogel@unifr.ch (D. Jaramillo-Vogel).

at the Oi-1. One of the rare sections where the EOT is recorded in shallow-water facies is found close to San Valentino (northern Italy). There, this biotic shift is characterized by a gradual disappearance of coralline algae and larger benthic foraminifera, parallel to a progressive increase in the percentage of bryozoan skeletons. In non-tropical carbonates, bryozoans are commonly dominant skeletal components (Collins, 1988; Nelson et al., 1988a,b; Bone and James, 1993; James et al., 1997; Hageman et al., 2000, 2003). However, a rise of the sea-surface temperature solely cannot trigger the disappearance from the neritic zone of coralline algae. Red algae also thrive in cool ocean waters (Pedley and Carannante, 2006; Büdenbender et al., 2011; Reid et al., 2011; Teichert et al., 2012). Therefore, additional environmental and/or ecological changes might have acted in combination with global cooling to induce the biofacies evolution recognized.

To better understand the mechanisms that produced this biotic change, a detailed microfacies analysis of the EOT interval was performed in the San Valentino section. Additionally, the total phosphorus content of the rock was measured in order to constrain the role of nutrients affecting the carbonate-producing organisms. The results are of significance in that they provide the shallow-water sedimentary expression of global environmental changes interpreted from deep-marine records, and, thus, may be compared with coeval shallow-water biofacies records from other basins worldwide.

2. Palaeogeographic and stratigraphic setting

The section outcropping near San Valentino village (Figs. 1, 2) belongs to the Calcare di Nago Formation (Castellarin and Cita, 1969a), which was deposited on the western margin of the Lessini Shelf, a Cenozoic carbonate platform superimposed on the Jurassic Trento platform (Bosellini, 1989; Luciani, 1989).

During the Late Eocene, the Lessini shelf was located within the subtropical belt at around 36° to 38°N (Meulenkamp and Sissingh, 2003). The San Valentino section has been previously interpreted by means of larger foraminifera as being of Priabonian (Late Eocene) age, based on the recognition of the *Nummulites fabianii* and *Nummulites retriatus* zones (Castellarin and Cita, 1969a). However, the uppermost part of the section (Fig. 2), which is difficult to access, was not examined in this latter publication.

The Calcare di Nago Formation is overlain by the Marne di Bolognano Formation. The base of this latter formation is Early Oligocene in age (Luciani, 1989), belonging to the P18 zone of Blow (1979) and Berggren et al. (1995). The transition between the Calcare di Nago and the Marne di Bolognano formations is not exposed near the section logged. It is however, responsible for the topographic step observed on Fig. 2A above the massive carbonates of the Calcare di Nago Formation (Luciani, 1989).

The carbonates analysed are mainly composed of open-marine phototrophic biota such as symbiont-bearing larger foraminifera and coralline algae (Luciani, 1989), with exception of the deposits outcropping in the uppermost part of San Valentino (above metre 110; Fig. 3), which are dominated by bryozoans, i.e., by heterotrophic organisms.

Bryozoan marls and limestones have long been known to develop around the Eocene–Oligocene boundary in south-central Europe (Braga, 1963, 1965, 1980; Braga and Barbin, 1987; Castellarin and Cita, 1969b; Setiawan, 1983; Barbin, 1988; Trevisani, 1997; Ungaro, 1978; Zágoršek, 1992, 1993, 1994, 1996, 2003; Braga et al., 1994; Zágoršek and Kázmér, 1999; Zágoršek and Darga, 2004; Nebelsick et al., 2005). In three sections outcropping about 40 km to the south-east of San Valentino (the Priabonian type locality Priabona, Buco della Rana, and Bressana), Setiawan (1983) reported the last occurrence of *Discocyclina* and *Asterocyclina* at the transition from larger foraminifera- to bryozoan-dominated deposits. This extinction is followed by an interval dominated by bryozoans (up to 100%). Above, *Operculina* and *Nummulites* re-occur. Similar to the observations made in the Priabona area (Setiawan, 1983), Castellarin and Cita (1969b) report broken discocyclinids at the base of a bryozoan limestone corresponding to the transition between the Calcare di Nago and the Marne di Bolognano formations at Val D'Ir (15 km north of San Valentino), which then completely disappear. Exactly the same evolution is observed in San Valentino, which suggests that the bryozoan beds were contemporaneous and had at least a regional extension (Fig. 4). This implies that, at

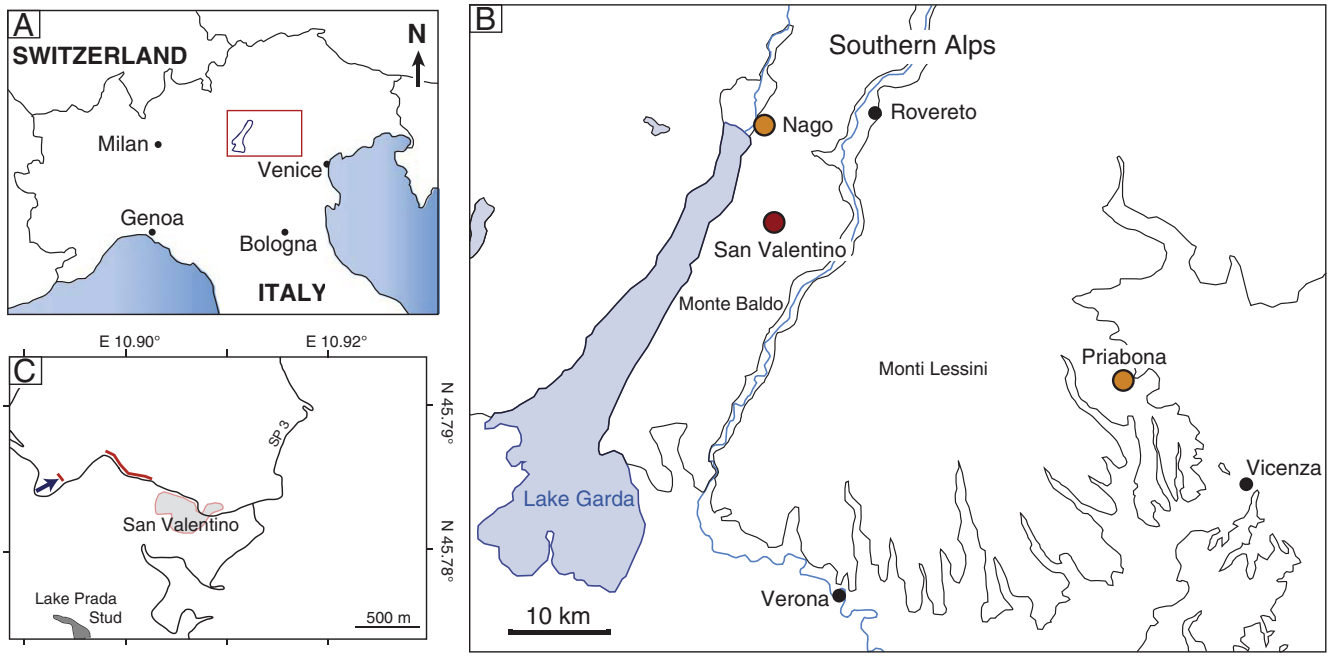

Fig. 1. A) Map of northern Italy showing the situation of the study area (red square). B) Magnification of the area marked with a red square in A displaying the environs of Monti Lessini and Lake Garda. The location of the Priabonian type locality at the town of Priabona and the type locality of the Calcare di Nago Formation at the town of Nago are pointed out with orange dots. The study presented herein was carried out in the outskirts of the village of San Valentino (red dot). C) Detailed map showing the location of the studied section (red lines) in San Valentino. The situation of the bryozoan beds of the upper part of the section is indicated with a blue arrow. Geographic coordinates are indicated.

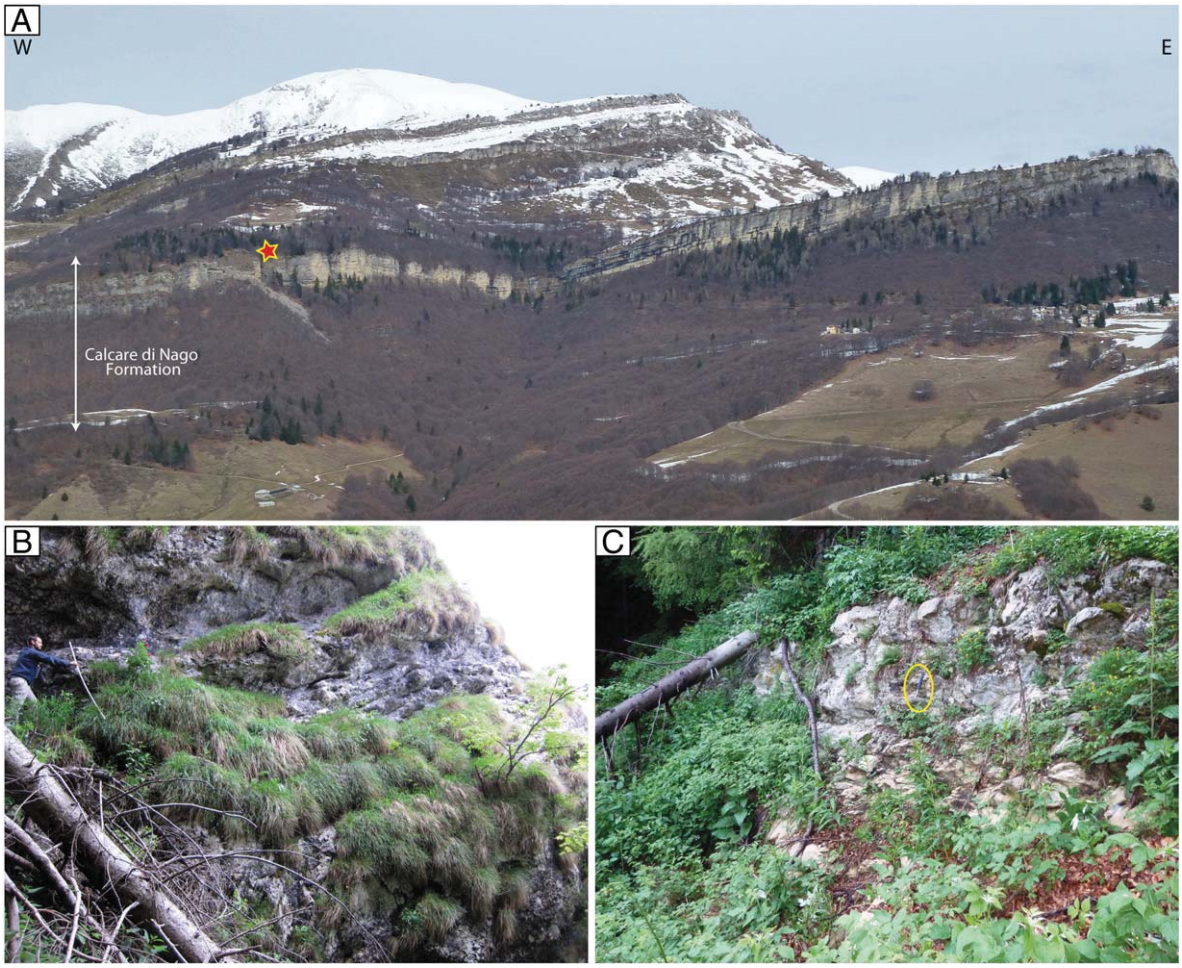

Fig. 2. A) Panoramic view of the Calcare di Nago Formation to the west of the village of San Valentino. The location of the bryozoan beds in the upper part of the San Valentino section is indicated with a star. Width of image is ca. 1 km. B) Outcrop view of the upper part of the San Valentino section logged along a gully in the cliff. Geologist = 1.78 m. C) Outcrop photograph of the bryozoan beds found in the upper part of the San Valentino section. Hammer encircled in yellow = 32 cm.

least regionally, the extinction of *Discocyclina* and *Asterocyclina* occurring together with the establishment of bryozoan beds as observed in San Valentino can be used for correlation.

By means of dinoflagellate cyst stratigraphy, Brinkhuis (1994) and Brinkhuis and Visscher (1995) were able to correlate the shallow-marine deposits of the Priabonian type locality (eastern Lessini Shelf, Fig. 1B) with pelagic sections of central Italy, including Massignano (Fig. 4). Following their correlation, the Eocene–Oligocene boundary as defined in Massignano occurs in the middle of the Priabonian type section. According to this correlation, the bryozoan beds occur about 10 m above the transposed Eocene–Oligocene boundary in the upper part of the Gse and the lower part of the Adi dinoflagellate cyst zones (Brinkhuis, 1994). This implies that the bryozoan beds and the extinction of discocyclinids in the Priabonian type locality occurred within the Early Oligocene.

3. Methods

The lower part of the San Valentino section (Figs. 2A, 3) was measured along the forest road SP3 (Strada Provinciale N. 3) to the west of the village of San Valentino (Fig. 1C; 45°47′8.16″N/10°53′57.12″E). From metre 88 upwards the section was measured along a gully in the cliff (Fig. 2A–B), directly before a tunnel (45°47′4.35″N/10°53′37.80″E). The lower part of the section is marly, tectonized, and partly covered. Therefore, only the upper part where the change in carbonate factory is recorded was sampled at a higher resolution. The outcrop ends at 123 metres and is overlain by a soil-covered depression. Additional accessible sections along the steep cliff (see Fig. 2A) formed by the Calcare di Nago Formation in the San Valentino area were not found. Therefore, unfortunately, the lateral facies evolution and a depositional model of the Calcare di Nago Formation in the study area cannot be reconstructed.

Seventy-two thin-sections were prepared in order to determine lithofacies. Point-counting was performed on 26 thin-sections (covering metres 91 to 124) in order to estimate the volume of the different particles in the interval containing the change in carbonate factory (Fig. 5). At least 600 points were counted in each thin-section with a grid spacing of 0.5 mm. Due to the large size-heterogeneity of the particles, a grid spacing had to be selected that is smaller than the size of the largest particles. This may lead to a slight overestimation of large particles. However, as coralline algae, larger foraminifera and bryozoan colonies are within a similar size range, this overestimation does not influence the relative abundance of these particles. All point-counting results were contrasted with observations made on the polished slabs in order to cross-check the representability of point-counting in the studied thin-sections. Pores in bioclasts filled with sediment or cement were counted as bioclasts (grain-bulk measurements sensu Jaanusson, 1972). Volume percent of bioclasts is given relative to the total of particles. Volume of cements and matrix is plotted separately. Fragments of red algae and of bryozoan colonies observed in the thin-sections are

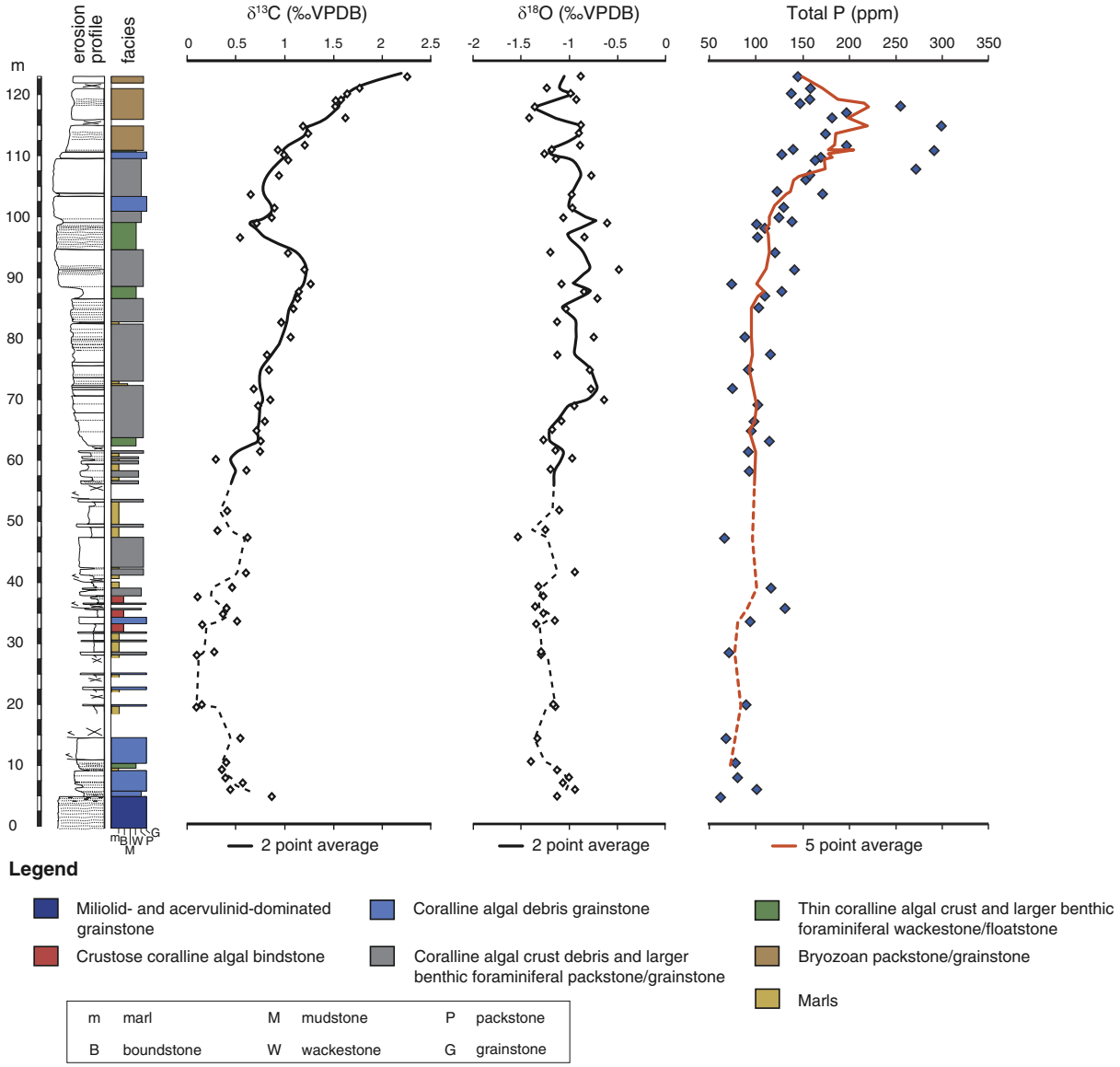

Fig. 3. Erosion profile and facies of the San Valentino section, together with the evolution of bulk $\delta^{13}C$, $\delta^{18}O$, and total phosphorus.

too small to permit taxonomic determinations. Cuts through the embryonic apparatus of larger foraminifera were not identified in the thin-sections, and thus were not determined at species level.

The carbon- and oxygen-isotope composition of 59 bulk samples was analysed (Fig. 3). The measurements were made on a FinniganMAT Delta Plus XL mass spectrometer equipped with an automated GasBench II at the Institute of Mineralogy and Geochemistry of the University of Lausanne (Switzerland). All results are reported in ‰ relative to the VPDB standard. The analytical reproducibility for three runs is better than ±0.1‰ for both $\delta^{13}C$ and $\delta^{18}O$.

For measuring the total phosphorus content (Fig. 3), 54 samples of the limestone beds were sawed and crushed to obtain powder. Around 100 mg powder was mixed with 0.5 ml $MgNO_3$ and dried in the oven for 30 min at 100 °C for each sample. Samples were then heated at 550 °C for 2.5 h. After cooling, 10 ml of 1 N HCl was added to each sample and left shaking for 16 h. The solutions were filtered (0.45 μm) and diluted ten times to be analysed using the ascorbic acid method of Eaton et al. (1995). The solution was mixed with ammonium molybdate and potassium antimonyl tartrate, which, in an acid medium, reacts with orthophosphate to form phosphomolybdic acid. This acid was then reduced with ascorbic acid to produce a blue colour. The intensity of the blue colour was determined with a photospectrometer (Perkin Elmer UV/Vis Photospectrometer Lambda 25). The concentration of PO_4 in mg/l was obtained by calibration with a known standard solution and converted to ppm. Individual samples/solutions were measured three times and precision was better than 5%. Replicate analyses of samples had a precision better than 5%. Samples with known concentration were measured and the precision was better than 10%.

4. Results

4.1. Facies evolution

The Calcare di Nago Formation is represented in the San Valentino area (Fig. 2A) by a thick (ca. 200 m) limestone succession overlaying volcanoclastic deposits. The basal interval (ca. 80 m, which was not logged) is composed of bedded packstones and grainstones dominated by geniculate and non-geniculate coralline algae and miliolid foraminifera. The studied interval starts at the transition between these rocks and lithofacies dominated by larger foraminifera and non-geniculate coralline algae (metre 5; Fig. 3). The facies described below are summarized in Table 1.

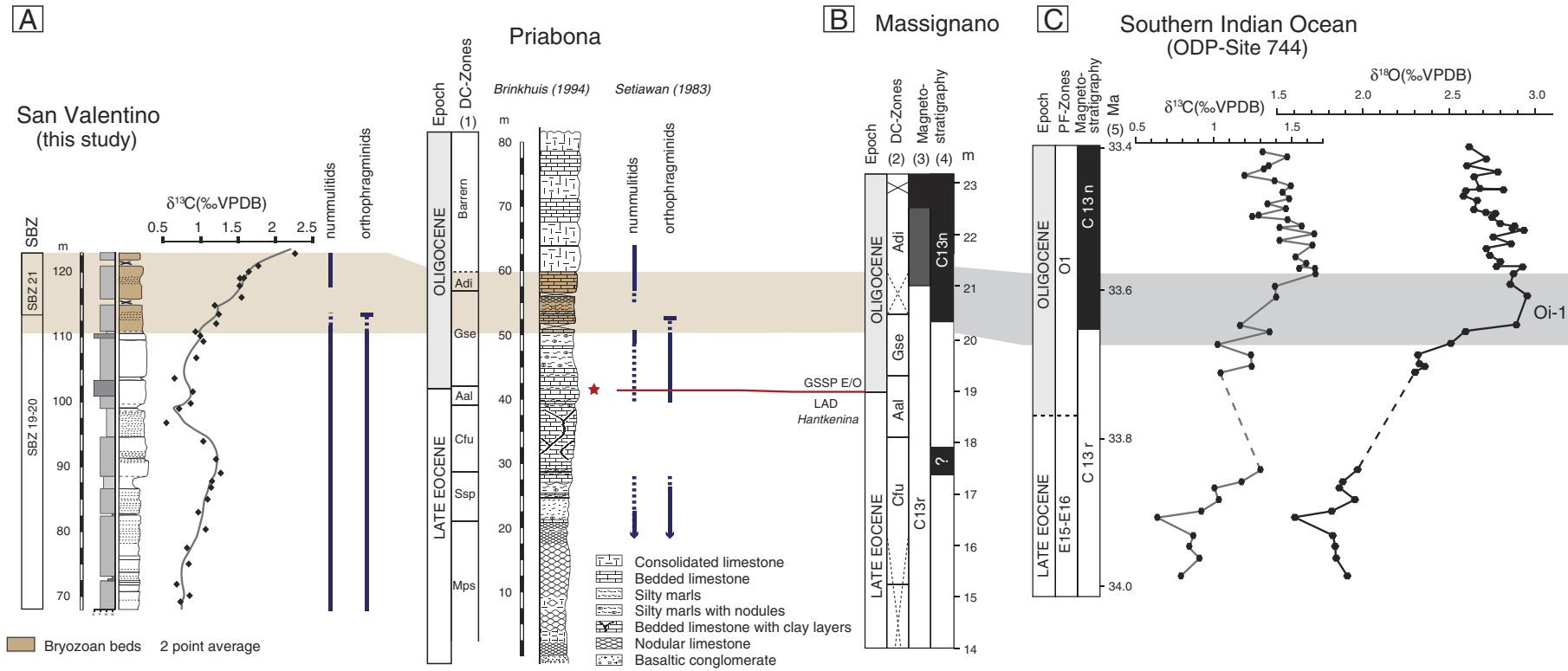

Fig. 4. A) Litho- and biostratigraphic correlation of the bryozoan beds of the upper part of the San Valentino section and of the Priabonian type locality at Priabona (brown-shaded area). Bulk rock stable carbon-isotope curve of San Valentino is plotted to the right of the section. Note the positive shift in carbon isotopes occurring within the bryozoan beds. Blue lines represent the distribution of orthophragminid (*Discocyclina* and *Asterocyclina*) and nummulitid (*Nummulites*, *Operculina*, *Heterostegina*) larger benthic foraminifera in both sections. *Discocyclina* and *Asterocyclina* disappear within the bryozoan beds, nummulitids (*Operculina* and *Nummulites*) re-occur within the upper part. Shallow benthic zonation in San Valentino (SBZ) is based on Castellarin and Cita (1969a) and Serra-Kiel et al. (1998). Dinoflagellate cyst zones in Priabona are from (1) Brinkhuis (1994). Red star indicates the position of the Eocene–Oligocene boundary in Priabona, as it was defined in Massignano (GSSP; Nocchi et al., 1988; Premoli Silva and Jenkins, 1993). B) Stratigraphy of the Massigano section displaying the dinoflagellate cyst biostratigraphy of (2) Brinkhuis and Biffi (1993). Magnetostratigraphy is after (3) Lowrie and Lanci (1994) and (4) Bice and Montanari (1988). Note that the bryozoan beds correspond to the transition between the Gse and Adi zones, which occurs at around the base of magnetochron C13n. C) Stratigraphy of ODP Site 744. Stable carbon- and oxygen-isotope curves measured on benthic foraminifera (*Cibicidoides* spp., Zachos et al., 1996). Dashed part of the curves corresponds to a 50 cm thick interval not sampled because of severe drilling disturbance. Age model (5) is based on conversion to Site 1218 (Coxall and Wilson, 2011). Note that the prominent positive oxygen-isotope shift leading to the Oi-1 occurs at the base of magnetochron C13n, shortly before a prominent carbon-isotope shift.

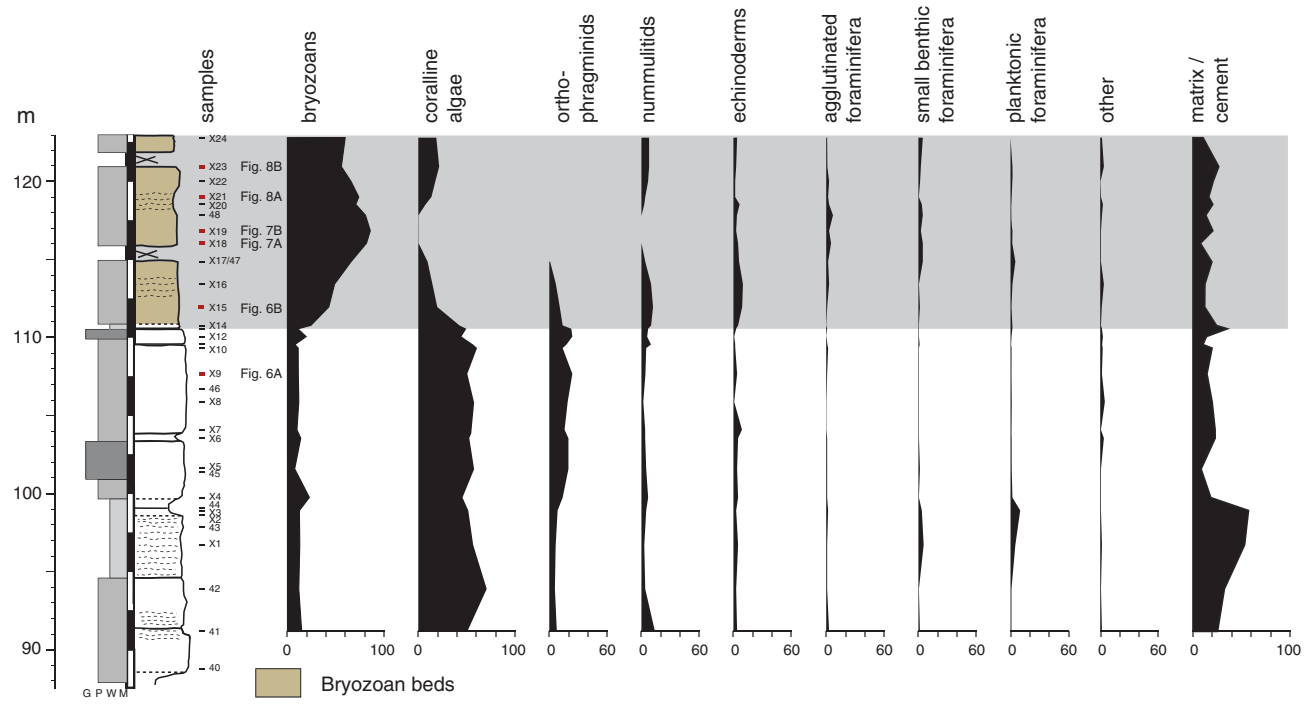

Fig. 5. Log of the upper interval of the San Valentino section containing the change in carbonate factory together with point-counting results. Black areas represent percentage of bioclasts. The percentage of matrix and cements is plotted separately. See Fig. 3 for legend.

The middle part of the section (15 to 62.5 m) is represented by marly intervals alternating with marly limestones and limestones. Around metre 50, marls and marly limestones contain coralline algal bindstones, which are the only autochthonous (non-reworked) components identified in the rocks studied, and extremely flat orthophragminids. From metre 62.5 upwards marly intervals decrease and the succession is again dominated by limestones displaying different proportions of larger foraminifera and coralline algae. At metre

Table 1
Facies description and interpretation of depositional environments.

Facies	Appearance in the field/fabric	Main constituents	Depositional environment
Miliolid- and acervulinid-dominated grainstone	Massive limestones, fine-grained, with rounded and well sorted grains	Small miliolids, *Borelis*, *Orbitolites*, asterigerinids, *Gypsina moussaviani*, *Chapmania*, *Halkyardia*, *Fabiania*, geniculate and non-geniculate coralline algal debris, phaceloid corals, echinoderm debris, rare *Nummulites* and discocyclinids.	High energy, shallow inner ramp
Crustose coralline algal bindstone	Wavy-bedded limestones and marly limestones: bindstone constructed by an open framework of thin coralline crusts	Thin coralline algal crusts (melobesioid-dominated association). Packstone to wackestone matrix contains larger foraminifera (*Discocyclina, Asterocyclina, Assilina alpina, Spirocypeus)* and bryozoans. Facies associated to sub-ellipsoidal and sub-discoidal rhodoliths (6 and 8 cm) with loosely packed laminar algal thalli with a high percentage of constructional voids	Low energy, outer ramp
Coralline algal debris grainstone	Massive limestone, highly bioturbated, components are sub-rounded to rounded, moderately- to well-sorted	Abraded non-geniculate red-algal debris and geniculate coralline algae, asterigerinids, small rotaliids, lense shaped *Nummulites* and *Discocyclina.* Less abundant are *Spiroclypeus*, *Heterostegina*, *Assilina alpina*, *Pellatispira maderazi* and *Asterocyclina.*	High energy, inner to middle ramp
Coralline algal crust debris and larger benthic foraminiferal packstone/grainstone	Massive limestone, highly bioturbated, components are angular, moderately- to very poorly-sorted	Thin red algal crust debris, rhodoliths, bryozoans, *Discocyclina*, *Asterocyclina*, *Pellatispira*, *Biplanispira*, *Heterostegina*, *Assilina alpina*, *Spiroclypeus* and *Nummulites.*	Moderate to low energy, middle to outer ramp
Thin coralline algal crust and larger benthic foraminiferal wackestone/floatstone	Wavy-bedded limestone with marly intercalations, highly bioturbated, up to 10 cm thick tempestite layers are intercalated	Thin coralline crusts (melobesioid-dominated association), orthophragminids (*Discocyclina* and *Asterocyclina*), bryozoans, planktonic foraminifera. Nummulitid foraminifera (*Spiroclypeus*, *Heterostegina*, *Assilina alpina*, *Pellatispira maderazi*) can be present.	Low energy, outer ramp
Bryozoan packstone/grainstone	Massive limestone beds, highly bioturbated, components are moderately well sorted	Bryozoan debris (up to 90%), echinoderms, non-geniculate red algae, agglutinated and planktonic foraminifera. In the lower part of the bryozoan beds a few broken operculinid and discocyclinid foraminifera filled with glauconite are present. In the upper part *Nummulites* and *Operculina* reoccur.	High energy, middle to outer ramp

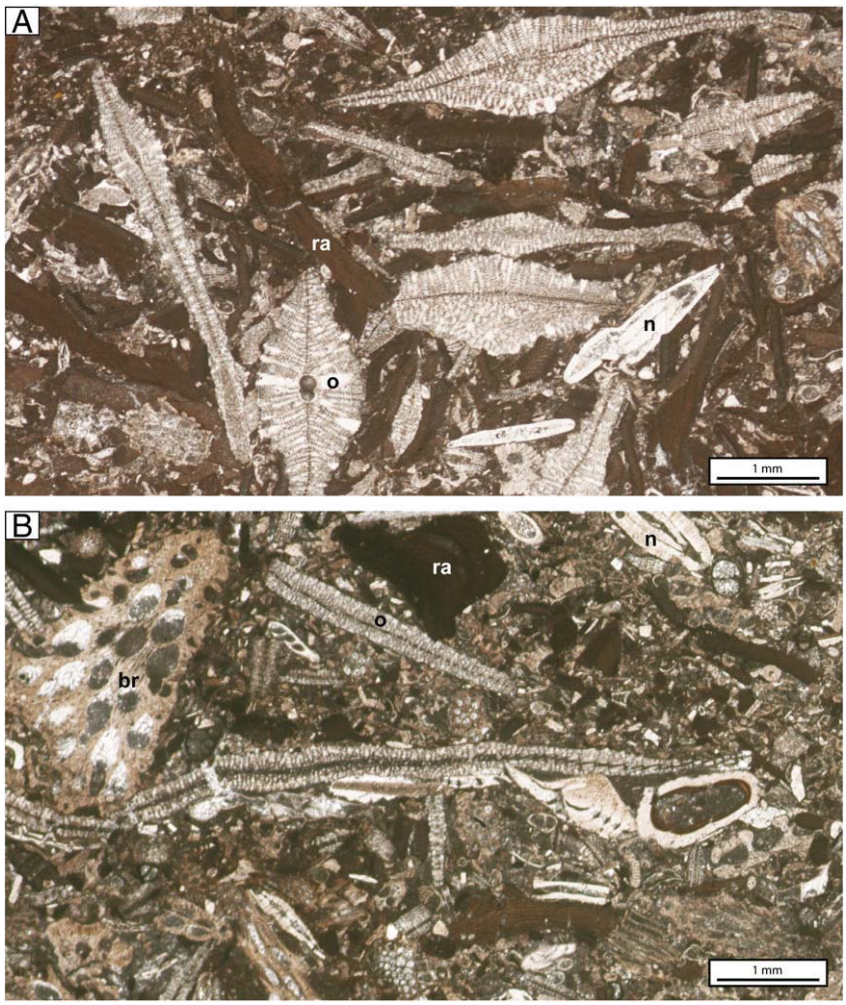

Fig. 6. Photomicrographs showing two different microfacies found between metre 107 and metre 116 in the upper part of the San Valentino section (Fig. 5). A) Packstone dominated by larger symbiont-bearing foraminifera (mainly orthophragminids but also nummulitids) and coralline algae (sample X9). B) Packstone corresponding to the lower part of the bryozoan beds. Note the presence of fragments of bryozoan colonies and red algae, as well as of orhtophragminid and nummulitid tests (sample X15). o = orthophragminid, n = nummulitid, br = bryozoan colony, ra = red alga.

110.8 a major change in biota is observed (Fig. 5). Lithofacies predominantly composed of coralline algae and larger foraminifera (Fig. 6A) are replaced by bryozoan-dominated limestones (Figs. 6B, 7).

Below metre 110.8, non-geniculate coralline algae clearly dominate the deposits (between 45 and 71% of total particles) (Figs. 5, 6A). The volume of orthophragminids (mainly *Discocyclina* and *Asterocyclina*) ranges between 6 and 24% with an increase above metre 99 (Fig. 6A), while nummulitids (*Nummulites*, *Operculina*, *Heterostegina*) make up not more than 14%. Bryozoans are present in all samples and reach up to 24%, while echinoderms just reach 9%. Planktonic foraminifera are significant (up to 10%) only within wackestones deposited between metres 95 and 100, where also small benthic foraminifera reach 6%. Agglutinated foraminifera do not surpass 3%.

Above metre 110.8 the proportion of bryozoan bioclasts rapidly rises (Figs. 5, 6B). The maximum concentration (up to 86%) is reached between metres 116 and 118 (Fig. 7). Coralline algae and orthophragminids, which dominate the deposits below, decrease rapidly and coevally to values below 1% in the case of red algae (strongly fragmented) and disappear completely in the case of orthophragminids. The last recognizable debris of *Asterocyclina* and *Discocyclina* is found at metre 114.8, indicating that orthophragminids disappeared somewhere between metres 110.8 and 114.8. The last occurrence of these larger foraminifera in San Valentino is tentatively placed at 113.5 m where the last moderately well preserved tests are found. At the base of the bryozoan-dominated beds, nummulitids increase slightly (up to 12%), together with echinoderms. However, nummulitids then decrease to less than 1%. The interval between metres 116 and 118 is characterized by the strong dominance of bryozoans (Fig. 7), only accompanied by small amounts of agglutinated foraminifera, small benthic foraminifera, planktonic foraminifera, and echinoderms. Nummulitids (*Operculina* and *Nummulites*) re-occur at metre 118.5 and reach 8% in the uppermost part of the section (Fig. 8). There, also red algae recover (22%), although the deposits remain dominated by bryozoans (Figs. 5, 8).

4.2. Stable isotopes (C and O) and phosphorus content

While the $\delta^{18}O$ values fluctuate between −0.5 and −1.5‰ throughout the studied section, the $\delta^{13}C$ curve shows a gently positive trend from ca. metre 20 to ca. metre 90 (Figs. 3, 4). Between metre 90 and metre 100, the $\delta^{13}C$ values display a negative spike of ~0.5‰. Above metre 100, a pronounced positive shift of almost 2‰ in C_{carb}-isotopic values occurs (Figs. 3, 4).

The total phosphorus contents of the limestone beds in the lower and middle part of the logged San Valentino section range between 62 and 141 ppm (Fig. 3). Mean values slightly increase from the lower part (~80 ppm) to the middle part (~100 ppm). In the upper part of the section, at around metre 100 (10 meters below the bryozoan

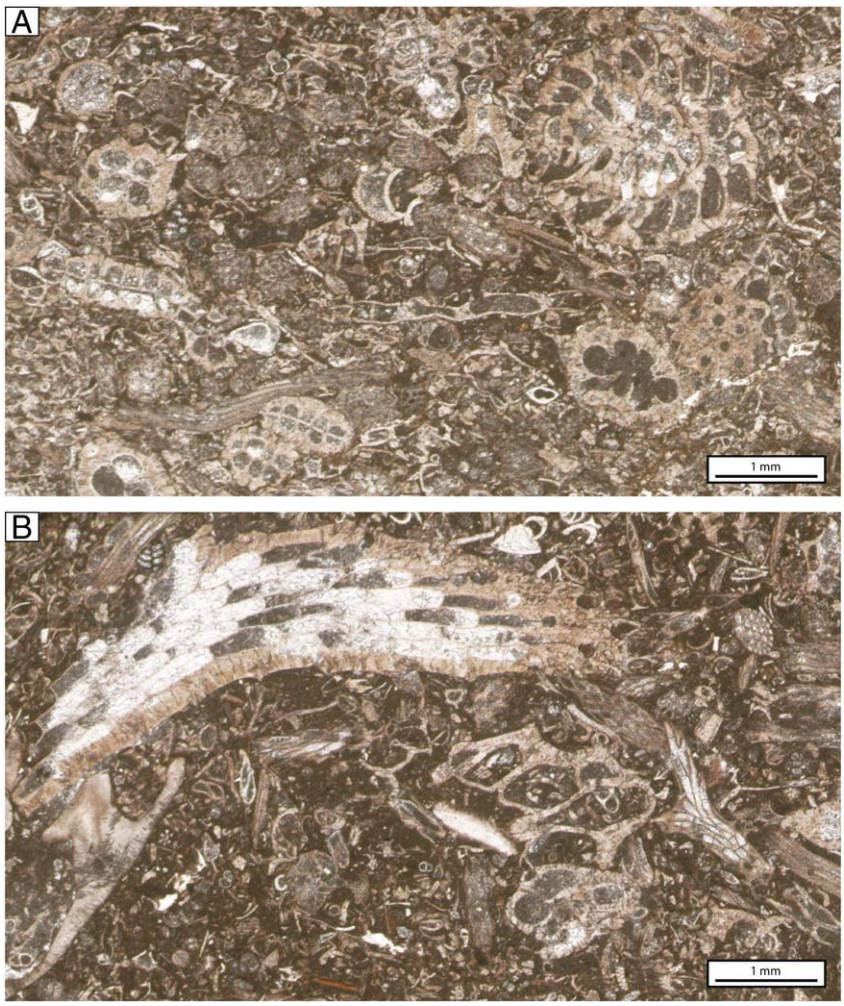

Fig. 7. Photomicrographs showing the bryozoan facies found between metre 116 and metre 118 in the upper part of the San Valentino section (Fig. 5). A) and B) Packstone textures containing more than 80% of bryozoans in the absence of larger benthic foraminifera and coralline algae (samples X18 and X19, respectively).

beds), total P contents increase rapidly and reach maximal values (300 ppm) within the bryozoan beds. Values start to decrease again around metre 118, in the upper part of the bryozoan beds.

5. Discussion

5.1. Change in carbonate factory

The majority of the rocks exposed in San Valentino are dominated by coralline algae and larger benthic foraminifera (Fig. 3). This is also the case for the 150 m thick shallow-marine succession outcropping in the Nago area (10 km north of San Valentino; Fig. 1B; Luciani, 1989; Jaramillo-Vogel et al., 2013;), which was deposited coevally with the middle and lower part of the San Valentino section. There, additionally to the coralline algae and larger foraminifera, hermatypic corals also occur (Bosellini, 1998).

Functional morphological studies of orthophragminids point to a general adaptation of these foraminifera to symbiosis with unicellular photosynthetic algae, as in nummulitid foraminifera (Ferràndez-Cañadell and Serra-Kiel, 1992; Ferràndez-Cañadell, 1998; Romero et al., 2002; Less and Özcan, 2008; Less et al., 2008). Most of the living symbiont-bearing larger foraminifera need mean annual water temperatures higher than 18 °C to support reproduction (Murray, 1973; Adams et al., 1986; Wilson and Vecsei, 2005). Furthermore, the majority of species of larger foraminifera are found in waters with mean summer temperatures above 25 °C (Wright and Murray, 1972) and are, therefore, confined to the tropical–subtropical belt (Adams et al., 1990). The majority of larger foraminifera species thrive in oligotrophic environments (Langer and Hottinger, 2000), although examples of slightly mesotrophic larger foraminifera-dominated facies have been described from modern carbonate platforms in the humid tropical belt or in tropical areas associated with nutrient upwelling (Wilson and Vecsei, 2005, and references therein).

The bryozoan beds in San Valentino are composed to a large part (and locally entirely) of light-independent organisms. While in modern environments phototrophs such as scleractinian corals and larger foraminifera are found in waters with winter surface temperatures above 20 °C (James, 1997), bryozoan-bearing heterotrophic communities dominate in cool waters (<20 °C) or in warm settings below the photic zone. Besides water temperature and light penetration, nutrients have an important influence on biotic carbonate production (Hallock and Schlager, 1986; Hallock, 2001; Pomar, 2001; Brandano and Corda, 2002; Mutti and Hallock, 2003; Halfar et al., 2004). While phototrophs, with the exception of red algae, need oligotrophic to slightly mesotrophic conditions to thrive, heterotrophic carbonate producers dominate in nutrient-rich settings (Hallock and Schlager, 1986; Hallock, 2001; Mutti and Hallock, 2003; Halfar et al., 2004, 2006; Wilson and Vecsei, 2005; Westphal et al., 2010).

Modern bryozoan-dominated deposits are common in the neritic zone of shelf and upper-slope settings in mid and high latitudes (Bader, 2001). As these organisms are light-independent, their deposits can form at depths of up to 1000 m (Henrich et al., 1992), although they

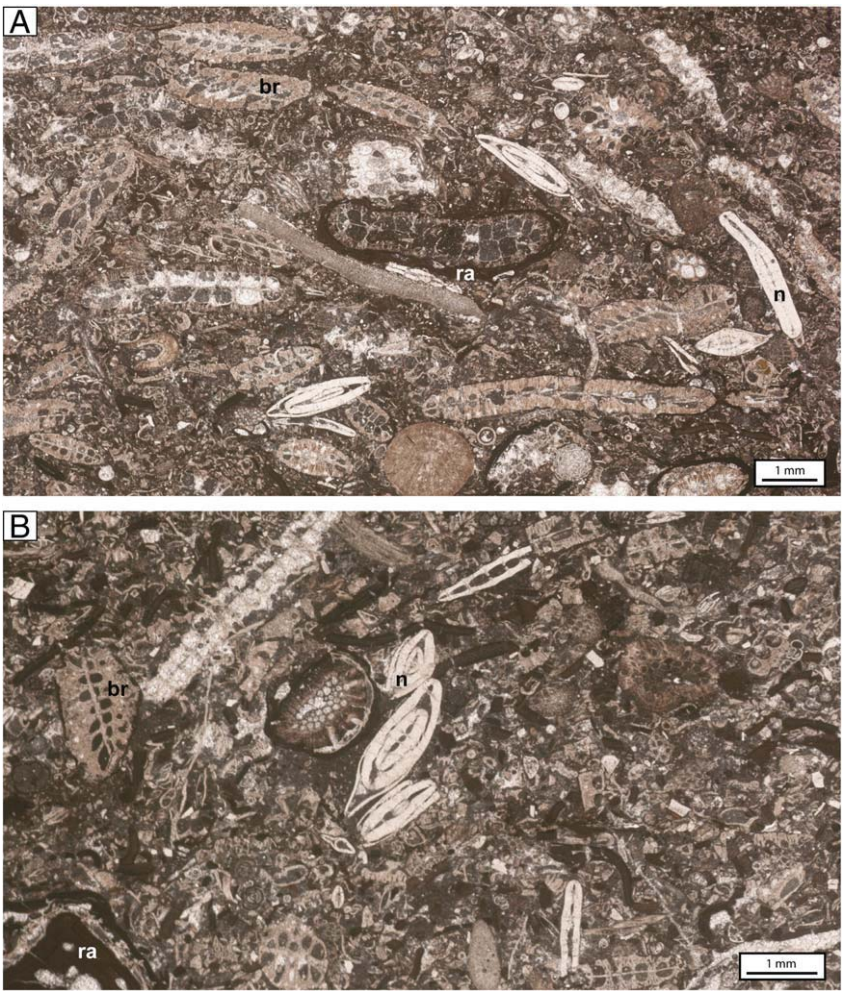

Fig. 8. Photomicrographs showing two different microfacies found above metre 118 in the upper part of the bryozoan beds (Fig. 5). A) Bryozoan-dominated packstone with few nummulitid foraminifera and coralline algae (sample X21). B) Packstone containing mainly nummulitid tests and fragments of bryozoan colonies and coralline algae (sample X23). n = nummulitid, br = bryozoan colony, ra = red alga.

are generally found at depths between 40 and 250 m (Halfar et al., 2006). They thrive in settings with an average annual temperature between 7 and 16 °C (Halfar et al., 2006, and references therein).

One explanation for the absence of light-dependent organisms and the deposition of bryozoan-dominated sediments would be a sudden deepening of the environment. However, the fact that this change in carbonate factory occurred coevally at different localities in northern Italy, which at the time of deposition were located at different palaeodepths (Setiawan, 1983), does not provide evidence for a depth-relation. Along these lines, an increased content in planktonic foraminifera would be expected in the bryozoan beds due to deepening. However, the facies in the uppermost part of the sedimentary record studied do not indicate such a rise in water depth (Fig. 5). Planktonic foraminifera exhibit their highest abundances below meter 100 of the section. Furthermore, facies analysis of the Calcare di Nago Formation in the San Valentino and Nago sections (Luciani, 1989; Jaramillo-Vogel et al., 2013) gives evidence for repetitive relative sea-level fluctuations recorded within these successions. The deepest facies recognized within the San Valentino section are located from metre 47.5 to metre 62.5 and are characterized by marls and limestones containing thin coralline algal crusts, thin larger foraminifera and planktonic foraminifera (Fig. 3 and Table 1). Bryozoan-dominated deposits occur neither within the entire Nago section (150 m) studied by Jaramillo-Vogel et al. (2013) nor in the middle and lower parts of the San Valentino succession (Fig. 3). Additionally, the disappearance of *Discocyclina* and *Asterocyclina*, which thrived in the lower part of the photic zone in outer platform settings (Romero et al., 2002; Beavington-Penney and Racey, 2004), within the bryozoan beds (Fig. 4) suggests a major environmental perturbation rather than a simple deepening of the depositional environment (see Cotton et al., 2014).

Conclusive evidence for a seawater temperature-related biotic change would require a taxonomic analysis at species level of the bryozoan colonies (e.g., Moisette, 2000) to discriminate between cool water, temperate and sub/tropical species. Such an analysis was not possible in the thin-sections examined due to the indurated nature of the calcareous material and the fragmented appearance of the bryozoan colonies preserved. However, based on observations in the modern Gulf of California, Halfar et al. (2004) concluded that heterozoan-dominated carbonates deposited in high-nutrient and high-temperature environments can be differentiated from heterozoan carbonates deposited in low-temperature settings because they contain 1 to 20% photozoan constituents, while true cold-water heterozoan associations contain less than 1% of photozoan organisms, irrespective of nutrient concentration. The middle part of the bryozoan beds in San Valentino consists of 100% heterotrophic organisms with up to 86% bryozoans (Figs. 5, 7), accompanied mainly by agglutinated and other small benthic foraminifera and echinoderms. Some levels of the bryozoan beds in Priabona (Figs. 1B, 4, 9) contain nearly 100% bryozoans (Setiawan, 1983). In

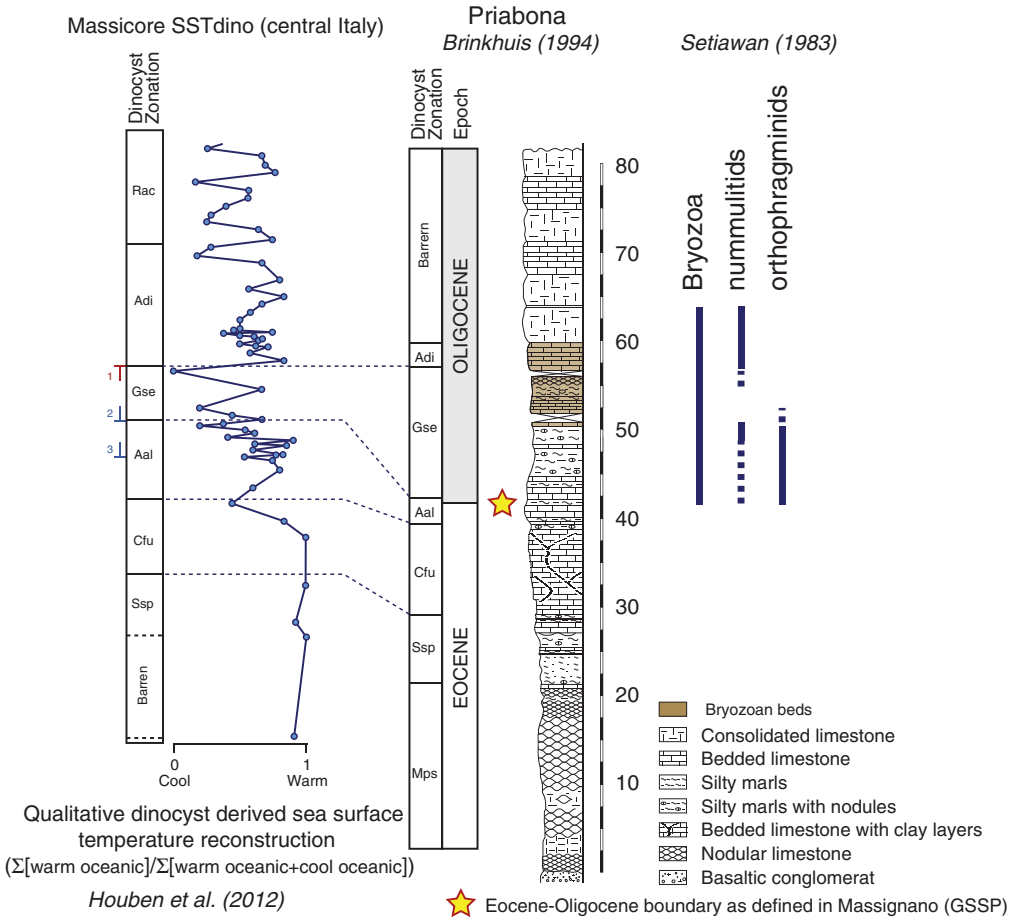

Fig. 9. Dinocyst zonation of the Priabona section (from Brinkhuis, 1994) plotted against the qualitative sea-surface temperature curve for the Late Eocene–Early Oligocene published by Houben et al. (2012). Note that from dinocyst Zone Cfu, but more clearly from Aal to Gse there is a relative cooling of the sea-surface temperature. Based on dinocyst stratigraphy the coolest interval corresponds to the bryozoan beds in Priabona and therefore in San Valentino, giving additional constrains that a sea-surface cooling occurred coevally with the development of bryozoan beds in northern Italy. The star marks the stratigraphic position of the Eocene–Oligocene boundary in Priabona, as it was defined in Massignano (GSSP; Nocchi et al., 1988; Premoli Silva and Jenkins, 1993). (1) Local disappearance of the dinoflagellate *Hemiplacophora semilunifera*, which corresponds to subtropical taxa. (2) and (3) introduction of the polar/boreal dinoflagellates *Glaphyrocysta semitecta* and *Lentina serrata*, respectively (Houben et al., 2012).

accordance with Halfar et al. (2004), the bryozoan beds recorded in northern Italy would thus correspond to a cold-water heterozoan association (sensu James, 1997).

Coralline algae can thrive in tropical to polar waters (Adey and Macintyre, 1973; Pedley and Carannante, 2006; Büdenbender et al., 2011; Reid et al., 2011; Teichert et al., 2012). The fact that red algae, which dominate in the 110 m long section underlying the bryozoan beds in San Valentino (Figs. 5, 6A), are virtually missing in the middle part of the bryozoan beds (max. 1% of fine red-algal debris) suggests that a further mechanism acted together with the cooling of ocean water, limiting coralline algal development during the deposition of the bryozoan beds.

5.2. Change in nutrient supply

Phosphorus represents an essential nutrient for living organisms. The distribution of phosphorus in sedimentary rocks has, therefore, been used as a proxy to estimate nutrient levels in ancient oceans (Föllmi, 1995, 1996; Van de Schootbrugge et al., 2003; Bodin et al., 2006; Mort et al., 2007; Godet et al., 2010). The flux of dissolved, bioavailable P into the oceans is mainly controlled by continental runoff and atmospheric transport (Föllmi, 1996; Delaney, 1998). The oceanic pathways of dissolved reactive P are dominated by primary productivity, export (sinking down) from the ocean surface, regeneration in the water column, and upwelling (Delaney, 1998).

There are no sedimentological evidences (e.g., hardgrounds, condensed intervals) to suggest that the increased P concentrations in the upper part of the section are the result of a lower sedimentation rate compared to the rest of the succession, which would have led to enrichment in P. The rise in phosphorus is gradual through the entire section and shows a more rapid increment at around metre 100, shortly below the bryozoan-dominated interval. The maximum values are reached within the middle part of the bryozoan beds, before decreasing again in the uppermost part of the section, still within the bryozoan facies (Fig. 3). Consequently, the higher P concentrations in the bryozoan beds are interpreted as resulting mainly from an increase in P accumulation rate.

A decrease in temperature could easily explain the absence of larger foraminifera within the bryozoan beds, but not the absence of coralline algae. Halfar et al. (2006) noted that in the Gulf of California, regardless of substrate type and temperature, two different carbonate factories develop: one dominated by coralline red algae with bryozoans being subordinate, and one dominated by bryozoans and molluscs. The coralline red algae-dominated association is supported by lower chlorophyll-α concentrations, lower amounts of dissolved inorganic nutrients, and a deeper euphotic zone. This suggests that the development of a bryomol assemblage versus a rhodalgal assemblage in the Gulf of California is

determined by nutrients rather than by temperature (Halfar et al., 2006). Also, in the Gulf of California, the coralline algal factories have lower P concentration in the water column compared to the bryomol factory (Halfar et al., 2006). Increased nutrient input into shallow waters causes plankton blooms and thus a shallowing of the photic zone due to increased turbidity, which could also have been responsible for the decline of coralline algae within the bryozoan beds. Therefore, it is well possible that, besides the temperature decrease, the shallowing of the photic zone also was an important factor leading to the decline of the symbiont-bearing orthophragminids.

In this regard, poorly illuminated shallow-water ecosystems with bryozoans dominating carbonate production occur in modern seas. For example, in Port Davey (south-west Tasmania), tannin mostly derived from hinterland vegetation blocks light penetration, and bryozoans dominate the sea bed as shallow as 10 m (Edgar et al., 2010; Shepherd and Edgar, 2014).

5.3. Stratigraphic position of the bryozoan beds

Based on the dinocyst biostratigraphy developed by Brinkhuis (1994) and Brinkhuis and Visscher (1995), the shallow-marine Priabonian type-locality can be correlated with the hemipelagic Massignano section where the GSSP for the Eocene–Oligocene boundary is defined (Fig. 4). Furthermore, based on the extinction of the orthophragminid foraminifera *Discocyclina* and *Asterocyclina* within the bryozoan beds in San Valentino as well as in Priabona (Setiawan, 1983), it is possible to correlate these two sections (Fig. 4). In Priabona, the bryozoan beds occur in the upper part of the Gse and the lower part of the Adi dinoflagellate cyst zones (Brinkhuis, 1994), about 10 m above the transposed Eocene–Oligocene boundary, which corresponds in Massignano to the interval around the base of magnetochron C13n. In the southern Indian Ocean, the positive $\delta^{18}O$ shift leading to the Oi-1 occurs at the base of C13n, prior to a positive shift of carbon-isotope values (Fig. 4).

Carbon-isotope values in San Valentino section show a pronounced positive shift above metre 100, roughly coinciding with the development of bryozoan dominated sediments. Although, it could be argued that the isotopic shift is the result of changing calcifying communities, the re-occurrence of larger foraminifera and coralline algae in the upper part of the section does not revert the trend (Figs. 3, 5) and, thus, an additional control must be invoked.

The use of carbon-isotope chemostratigraphy has become a powerful tool for chronostratigraphic correlations between platform and pelagic sections (Jenkyns, 1995; Vahrenkamp, 1996; Ferreri et al., 1997; Grötsch et al., 1998; Menegatti et al., 1998; Stoll and Schrag, 2000; Mutti et al., 2006; Parente et al., 2007; Burla et al., 2008; Huck et al., 2011). Therefore, based on its stratigraphic location, the positive $\delta^{13}C$ shift occurring in the upper part of San Valentino (Figs. 3, 4) can be interpreted to correspond to the positive shift around C13n in deep-sea records. Although the $\delta^{18}O$ values from San Valentino do not show any clear trends that would translate a global signal, the correlation of the positive $\delta^{13}C$ shift implies that the climate shift leading to the Oi-1 must correspond approximately to the base of the bryozoan beds.

5.4. Regional shallow-marine response to a global change?

The sedimentary record on the New Jersey shelf spanning the Oi-1 exhibits evidence of a eustatic sea-level fall of around 55 m (Kominz and Pekar, 2001; Miller et al., 2009). Based on microfacies, sedimentological and biotic analysis, Houben et al. (2012) interpreted a sea-level fall of 50 to 60 m at the end of deposition of the bryozoan beds in Priabona. However, no physical evidence for an emersion surface that would indicate a sea-level fall has been found in San Valentino (possibly due to the fact that in the upper part of the studied interval some bed limits are covered; Figs. 2B–C, 3). Miller et al. (2009) suggested that this sea-level drop was accompanied by a drop in sea-surface temperature of 1.5 to 2 °C. This is in agreement with a cooling of around 2 °C inferred by the Mg/Ca ratio of benthic foraminifera from St. Stephens Quarry (Alabama, USA; Wade et al., 2012). However, Lear et al. (2004, 2008) did not find evidence for a temperature drop at the Oi-1 based on the Mg/Ca record of ODP Site 1218 in the Pacific Ocean, which implies that there are contradictory data and interpretations concerning the temperature change at the Oi-1.

A sea-surface temperature curve was produced based on dinocysts in the Massicore, a core drilled around 100 m away from the Massignano section (the GSSP locality for the Eocene–Oligocene boundary; see Montanari et al., 1994), which is around 300 km to the sourth of San Valentino. Quantitative analyses of warm-oceanic vs. cool-oceanic dinocyst distribution in the Massicore resulted in a qualitative sea-surface temperature proxy for the EOT (Fig. 9; Houben et al., 2012). This proxy suggests a cooling maximum within the upper part of the Gse dinocyst zone, which coincides with the lower part of the bryozoan beds in Priabona (Fig. 9; Brinkhuis, 1994) and, consequently, in San Valentino (Fig. 4). This evolution is underlined by the appearance of taxa formerly only recorded in boreal and polar regions: *Lentina serrata* and *Glaphyrocysta semitecta* occur within the Aal dinocyst zone and at the transition between Aal and Gse, respectively (Fig. 9). Also, there is a regional disappearance of typical subtropical taxa like *Hemiplacophora semilunifera* at the transition between the Gse and Adi zones (Houben et al., 2012). According to our stratigraphic scheme (Fig. 4), this corresponds to the interval of the Oi-1 and thus provides evidence for a cooling of ocean surface waters during the Oi-1 in this palaeogeographic region. The subsequent warming at the base of the Adi zone could account for the partial recovery of the carbonate factory, with the reappearance of nummulitid foraminifera in the upper part of the bryozoan beds.

Deep-sea records suggest an increase in ocean surface palaeoproductivity occurring coevally to the $\delta^{18}O$ shift at the EOT, especially in the Southern Ocean but also in mid and low latitudes (Diester-Haass, 1996; Diester-Haass and Zahn, 1996; Salamy and Zachos, 1999; Diester-Haass and Zachos, 2003; Dunkley Jones et al., 2008; Wade and Pearson, 2008; Coxall and Wilson, 2011; Plancq et al., 2014; Villa et al., 2014). This change is characterized by an important increase in export production shown by an increase in accumulation rate of benthic and planktonic foraminifera, radiolarians, diatoms, fish debris, echinoderms, and ostracodes (Coxall and Pearson, 2007, and references therein). Records of the Southern Ocean suggest a several-fold increase in primary productivity in response to the Oi-1 (Baldauf and Barron, 1990; Baldauf, 1992; Salamy and Zachos, 1999). In the eastern equatorial Pacific, the Eocene–Oligocene climate change did not trigger a major shift towards increased productivity, but there is evidence for a short-lived rise in productivity and export production associated to the onset of sustained Antarctic glaciation (Coxall and Wilson, 2011). The increase in benthic foraminifera accumulation rate in the eastern equatorial Pacific and coeval opal accumulation in the Southern Ocean suggest that there is a link between both sites (Coxall and Wilson, 2011), such as an intensification of thermohaline circulation as interpreted for the earliest Oligocene (Miller and Tucholke, 1983; Wright and Miller, 1993; Thomas et al., 2008; Cramer et al., 2009; Coxall and Wilson, 2011; Pusz et al., 2011).

The positive $\delta^{13}C$ shift near the Oi-1 lags behind the shift in $\delta^{18}O$ (Fig. 4). Salamy and Zachos (1999) therefore suggest a cause-and-effect relationship. The trend towards higher net productivity interpreted to be due to intensification and expansion of upwelling systems may have elevated the export flux of C_{org} to sediments during the Early Oligocene (Zachos et al., 1996), being responsible for the observed rise in mean ocean $\delta^{13}C$ (Salamy and Zachos, 1999).

The cause of worldwide increase in palaeoproductivity from the Late Eocene to the Oligocene is interpreted to have been induced by ocean mixing and circulation changes that increased the availability of nutrients in surface waters, although the mechanism producing these

changes is still matter of debate (Diester-Haass and Zahn, 1996; Salamy and Zachos, 1999; Diester-Haass and Zachos, 2003; Coxall and Pearson, 2007).

Interestingly, the increase in phosphorus in San Valentino is associated to the earliest Oligocene positive shift in $\delta^{13}C$ (Figs. 3, 4). This suggests that there was a link between the rise in productivity as recorded in deep-sea successions and the increase in phosphorus content, and that this was reflected by the formation of the bryozoan beds in the shallow-water realm of northern Italy.

6. Conclusions

Detailed facies analysis of the Calcare di Nago Formation in northern Italy has revealed a drastic change in shallow-water carbonate factory occurring at around the Eocene–Oligocene transition. In the San Valentino section, red algae and larger benthic foraminifera dominate in the lower part of the section, while its uppermost part is composed of bryozoan-rich beds. This replacement of phototrophic by heterotrophic organisms implies a significant change in the environmental conditions. The disappearance of *Discocyclina* and *Asterocyclina* occurring together with the establishment of bryozoan beds can be used for correlation with the Priabonian section, which was correlated by means of dinocyst biostratigraphy to deep-marine sections. Furthermore, there is a significant positive shift in $\delta^{13}C$ that starts just below the bryozoan beds. This allows correlation with published deep-water records and thus permits discussing the reasons for this change affecting the carbonate-producing organisms.

Global cooling of sea-surface temperature linked to the earliest Oligocene glaciation (Oi-1) was not the only mechanism triggering the disappearance of larger foraminifera and coralline algae from the neritic realm in northern Italy. The change in trophic resources around the Oi-1, recognized in deep-sea records and indicated by a rise in total phosphorus content in the platform carbonates investigated, is interpreted to have played a part increasing primary productivity and, thus, producing a shallowing of the photic zone. Decreased water transparency would have limited light-dependent biota and left bryozoans as dominant benthic calcifying organisms. The coeval deposition of bryozoan beds reported from several localities in northern Italy is interpreted to represent the regional reaction of a carbonate platform depositional system to global oceanographic changes related to the beginning of the Antarctic glaciation.

Acknowledgements

Jochen Halfar and two anonymous reviewers are thanked for reviewing an earlier version of this manuscript. Karl Föllmi and Thierry Adatte (University of Lausanne) are thanked for offering their laboratory for P analysis. The financial support of the Swiss National Science Foundation (grant 20-121545) and the Grup de recerca reconegut per la Generalitat de Catalunya 2014 SGR 251 “Geologia Sedimentària” is gratefully acknowledged.

References

Adams, C.G., Butterlin, J., Samanta, B.K., 1986. Larger foraminifera and events at the Eocene/Oligocene boundary in the Indo-West Pacific region. In: Pomerol, C., Premoli Silva, I. (Eds.), Terminal Eocene EventsDevelopments in Palaeontology and Stratigraphy 9. Elsevier Science Ltd., pp. 237–252.

Adams, C.G., Lee, D.E., Rosen, B.R., 1990. Conflicting isotopic and biotic evidence for tropical sea-surface temperatures during the Tertiary. Palaeogeography, Palaeoclimatology, Palaeoecology 77, 289–313.

Adey, W.H., Macintyre, I.G., 1973. Crustose coralline algae — re-evaluation in geological sciences. Geological Society of America Bulletin 84, 883–904.

Bader, B., 2001. Modern bryomol-sediments in a cool-water, high-energy setting: the inner shelf off northern Brittany. Facies 44, 81–103.

Baldauf, J.G., 1992. Middle Eocene through early Miocene diatom floral turnover. In: Prothero, D.R., Berggren, W.A. (Eds.), Eocene–Oligocene Climatic and Biotic Evolution. Princeton University Press Princeton, New Jersey, pp. 310–326.

Baldauf, G., Barron, A., 1990. Evolution of biosiliceous sedimentation patterns — Eocene through Quatemary: paleoceanographic response to polar cooling. In: Bleil, U., Thiede, R. (Eds.), Geological History of the Polar Oceans: Arctic versus Antarctic. Kluwer Academic, Norwell, MA, pp. 575–607.

Barbin, V., 1988. The Eocene–Oligocene transition in shallow-water environment: the Priabonian stage type area (Vicentin, northern Italy). In: Premoli Silva, I., Coccioni, R., Montanari, A. (Eds.), The Eocene–Oligocene Boundary in the Marche-Umbria Basin (Italy)Special Publication International Subcommission on Paleogene Stratigraphy. IUGS, Ancona, pp. 163–171.

Beavington-Penney, S.J., Racey, A., 2004. Ecology of extant nummulitids and other larger benthic foraminifera: applications in palaeoenvironmental analysis. Earth-Science Reviews 67, 219–265.

Berggren, W.A., Kent, D.V., Swisher, C.C., Aubry, M.P., 1995. A revised Cenozoic geochronology and chronostratigraphy. SEPM Special Publication 54, 129–212.

Bice, D.M., Montanari, A., 1988. Magnetic stratigraphy of the Massignano section across the Eocene–Oligocene boundary. In: Premoli Silva, I., Coccioni, R., Montanari, A. (Eds.), The Eocene–Oligocene Boundary in the Marche-Umbria Basin (Italy)Special Publication International Subcommission on Paleogene Stratigraphy. IUGS, Ancona, pp. 111–117.

Blow, W.H., 1979. The Cenozoic Globigerinida: a study of the morphology, taxonomy, evolutionary relationships and the stratigraphical distribution of some Globigerinida (mainly Globigerinacea). 3 vols. E.J. Brill, Leiden (1413 pp.).

Bodin, S., Godet, A., Föllmi, K.B., Vermeulen, J., Arnaud, H., Strasser, A., Fiet, N., Adatte, T., 2006. The late Hauterivian Faraoni oceanic anoxic event in the western Tethys: evidence from phosphorus burial rates. Palaeogeography, Palaeoclimatology, Palaeoecology 235, 245–264.

Bone, Y., James, N.P., 1993. Bryozoans as carbonate sediment producers on the cool-water Lacepede Shelf, southern Australia. Sedimentary Geology 86, 247–271.

Bosellini, A., 1989. Dynamics of Tethyan carbonate platforms. In: Crevello, P.D., Wilson, J.L., Sarg, J.F., Read, J.F. (Eds.), Controls on Carbonate Platform and Basin Development. SEPM Special Publication 44, pp. 3–13.

Bosellini, F.R., 1998. Diversity, composition and structure of Late Eocene shelf-edge coral associations (Nago Limestone, Northern Italy). Facies 39, 203–225.

Braga, G., 1963. Il briozoi del Terziario Veneto. Bollettino della Societa Paleontologica Italiana 2 (1), 16–55.

Braga, G., 1965. Briozoi dell'Oligocene di Possagno (Trevigiano occidentale). Il contributo all conoscenza dei briozoi del Terziario veneto. Bollettino della Societa Paleontologica Italiana 4 (2), 216–244.

Braga, G., 1980. Il briozoi dei dintorni di Rovereto. Monte Baldo settentrionale e Valle di GrestaMuseo Civico di Rovereto, Pubblicazione 82 (103 pp.).

Braga, G., Barbin, V., 1987. Bryozoaries du Priabonien stratotypique (Province Vicenza, Italie). Revue du Paléobiologie 7 (2), 495–556.

Braga, G., Kázmér, K., Zágoršek, K., 1994. Comparison between Venetian and Western Carpathians Late Eocene bryozoan faunas. Proceedings from Shallow Tethys 4, 24–41.

Brandano, M., Corda, L., 2002. Nutrients, sea level and tectonics: constrains for the facies architecture of a Miocene carbonate ramp in central Italy. Terra Nova 14, 257–262.

Brinkhuis, H., 1994. Late Eocene to Early Oligocene dinoflagellate cysts from the Priabonian type-area (Northeast Italy) — biostratigraphy and paleoenvironmental interpretation. Palaeogeography, Palaeoclimatology, Palaeoecology 107, 121–163.

Brinkhuis, H., Biffi, U., 1993. Dinoflagellate cyst stratigraphy of the Eocene/Oligocene transition in central Italy. Marine Micropaleontology 22, 131–183.

Brinkhuis, H., Visscher, H., 1995. The upper boundary of the Eocene Series: a reappraisal based on dinoflagellate cyst biostratigraphy and sequence stratigraphy. In: Berggren, W.A., Kent, D.V., Swisher, C.C., Aubry, M.P., Hardenbol, J. (Eds.), Geochronology, Time Scales and Global Stratigraphic Correlations: A Unified Temporal Framework for an Historical Geology. SEPM Special Publication 54, pp. 295–304.

Büdenbender, J., Riebesell, U., Form, A., 2011. Calcification of the Arctic coralline red algae *Lithothamnion glaciale* in response to elevated CO_2. Marine Ecology Progress Series 441, 79–87.

Burla, S., Heimhofer, U., Hochuli, P.A., Weissert, H., Skelton, P., 2008. Changes in sedimentary patterns of coastal and deep-sea successions from the North Atlantic (Portugal) linked to Early Cretaceous environmental change. Palaeogeography, Palaeoclimatology, Palaeoecology 257, 38–57.

Castellarin, A., Cita, M.B., 1969a. Calcare di Nago. – Studi Ill. Carta Geologica d'Italia, Formazioni Geologiche, Roma, fascicolo 2, 49–64.

Castellarin, A., Cita, M.B., 1969b. La coupe priabonienne de Nago (Prov. Trento) et la limite Eocene–Oligocene. Colloque sur l'Eocène, Mémoire du Bureau de Recherches Géologiques et Minières (B.R.G.M.) 69 pp. 93–117.

Collins, L.B., 1988. Sediments and history of the Rottnest Shelf, southwest Australia: a swell-dominated, non-tropical carbonate margin. Sedimentary Geology 60, 15–49.

Cotton, L.J., Pearson, P.N., Renema, W., 2014. Stable isotope stratigraphy and larger benthic foraminiferal extinctions in the Melinau Limestone, Sarawak. Journal of Asian Earth Sciences 79, 65–71.

Coxall, H.K., Pearson, P.N., 2007. The Eocene–Oligocene transition. In: William, M., Haywood, A.M., Gregory, F.J., Schmidt, D.N. (Eds.), Deep-Time Perspectives on Climate Change: Marrying the Signal from Computer Models and Biological Proxies. The Micropaleontological Society Special Publications, London, pp. 351–387.

Coxall, H.K., Wilson, P.A., 2011. Early Oligocene glaciation and productivity in the eastern equatorial Pacific: insights into global carbon cycling. Paleoceanography 26, PA2221. http://dx.doi.org/10.1029/2010PA002021.

Cramer, B.S., Toggweiler, J.R., Wright, J.D., Katz, M.E., Miller, K.G., 2009. Ocean overturning since the Late Cretaceous: inferences from a new benthic foraminiferal isotope compilation. Paleoceanography 24, PA4216. http://dx.doi.org/10.1029/2008PA001683.

Delaney, M.L., 1998. Phosphorus accumulation in marine sediments and the oceanic phosphorus cycle. Global Biogeochemical Cycles 12, 563–572.

Diester-Haass, L., 1996. Late Eocene–Oligocene paleoceanography in the southern Indian Ocean (ODP Site 744). Marine Geology 130, 99–119.
Diester-Haass, L., Zachos, J., 2003. The Eocene–Oligocene Transition in the Equatorial Atlantic (ODP Site 925): paleoproductivity increase and positive $\delta^{13}C$ excursion. In: Prothero, D.R., Ivany, L.C., Nesbitt, E.A. (Eds.), From Greenhouse to Icehouse: The Marine Eocene–Oligocene Transition. Columbia University Press, New York, pp. 397–416.
Diester-Haass, L., Zahn, R., 1996. Eocene–Oligocene transition in the Southern Ocean: history of water mass circulation and biological productivity. Geology 24, 163–166.
Dunkley Jones, T., Bown, P.R., Pearson, P.N., Wade, B.S., Coxall, H.K., Lear, C.H., 2008. Major shifts in calcareous phytoplankton assemblages through the Eocene-Oligocene transition of Tanzania and their implications for low-latitude primary production. Paleoceanography 23, PA4204. http://dx.doi.org/10.1029/2008PA001640.
Eaton, A.D., Clesceri, L.S., Greenberg, A.E., 1995. Standard Methods for the Examination of Water and Wastewater. 19th edition. American Public Health Association, Washington (1100 pp.).
Edgar, G.J., Last, P.R., Barret, N.S., Gowlett-Holmes, K., Driessen, M., Mooney, P., 2010. Conservation of natural wilderness values in the Port Davey marine and estuarine protected area, south-western Tasmania. Aquatic Conservation: Marine Freshwater Ecosystems 20, 297–311.
Ferràndez-Cañadell, C., 1998. Morphostructure and paleobiology of Mesogean orthophragminids (Discocyclinidae and Orbitoclypeidae, Foraminifera). Acta Geologica Hispánica 31, 183–187.
Ferràndez-Cañadell, C., Serra-Kiel, J., 1992. Morphostructure and paleobiology of Discocyclina Gümbel, 1870. Journal of Foraminiferal Research 22, 147–165.
Ferreri, V., Weissert, H., d'Argenio, B., Buonocunto, F.P., 1997. Carbon isotope stratigraphy: a tool for basin to carbonate platform correlation. Terra Nova 9, 57–61.
Föllmi, K.B., 1995. 160 m.y. record of marine sedimentary phosphorus burial: coupling of climate and continental weathering under greenhouse and icehouse conditions. Geology 23, 503–506.
Föllmi, K.B., 1996. The phosphorus cycle, phosphogenesis and marine phosphate-rich deposits. Earth-Science Reviews 40, 55–124.
Godet, A., Föllmi, K.B., Bodin, S., de Kaenel, E., Matera, V., Adatte, T., 2010. Stratigraphic, sedimentological and palaeoenvironmental constraints on the rise of the Urgonian platform in the western Swiss Jura. Sedimentology 57, 1088–1125.
Grötsch, J., Billing, I., Vahrenkamp, V., 1998. Carbon isotope stratigraphy in shallow water carbonates: implications for Cretaceous black shale deposition. Sedimentology 45, 623–634.
Hageman, S.J., James, N.P., Bone, Y., 2000. Cool-water carbonate poduction from epizoic bryozoans on ephemeral substrates. Palaios 15, 33–48.
Hageman, S.J., Lukasik, J., McGowran, B., Bone, Y., 2003. Paleoenvironmental significance of *Celleporaria* (Bryozoa) from modern and Tertiary cool-water carbonates of Southern Australia. Palaios 18, 510–527.
Halfar, J., Godinez-Orta, L., Mutti, M., Valdez-Holguín, J.E., Borges, J.M., 2004. Nutrient and temperature controls on modern carbonate production: an example from the Gulf of California, Mexico. Geology 32, 213–216.
Halfar, J., Strasser, M., Riegl, B., Godinez-Orta, L., 2006. Oceanography, sedimentology and acoustic mapping of a bryomol carbonate factory in the northern Gulf of California, Mexico. In: Pedley, H.M., Carannante, G. (Eds.), Cool-Water Carbonates: Depositional Systems and Palaeoenvironmental Controls. Geological Society, London, Special Publications 255, pp. 197–215.
Hallock, P., 2001. Coral reefs, carbonate sediments, nutrients, and global change. In: Stanley, G.D. (Ed.), The History and Sedimentology of Ancient Reef Systems. Kluwer Academic/Plenum Publishers, New York, pp. 387–427 (Springer).
Hallock, P., Schlager, W., 1986. Nutrient excess and the demise of coral reefs and carbonate platforms. Palaios 1, 389–398.
Henrich, R., Hartmann, M., Reitner, J., Schäfer, P., Freiwald, A.S., 1992. Facies belts and communities of the Arctic Vesterisbanken Seamount (Central Greenland Sea). Facies 27, 71–1043.
Houben, A.J.P., Van Mourik, C.A., Montanari, A., Coccioni, R., Brinkhuis, H., 2012. The Eocene–Oligocene transition: changes in sea level, temperature or both? Palaeogeography, Palaeoclimatology, Palaeoecology 335, 75–83.
Huck, S., Heimhofer, U., Rameil, N., Bodin, S., Immenhauser, A., 2011. Strontium and carbon-isotope chronostratigraphy of Barremian–Aptian shoal-water carbonates: Northern Tethyan platform drowning predates OAE 1a. Earth and Planetary Science Letters 304, 547–558.
Jaanusson, V., 1972. Constituent analysis of an Ordovician limestone from Sweden. Lethaia 5, 217–237.
James, N.P., 1997. The cool-water carbonate depositional realm. In: James, N.P., Clarke, J.A.D. (Eds.), Cool-water Carbonates 56. SEPM Special Publication, Tulsa, pp. 1–22.
James, N.P., Bone, Y., Hageman, S.J., Feary, D.A., Gostin, V.A., 1997. Cool-water carbonate sedimentation during the terminal Quaternary sea-level cycle: Lincoln Shelf, southern Australia. In: James, N.P., Clarke, J.A.D. (Eds.), Cool-water Carbonates 56. SEPM Special Publication, Tulsa, pp. 53–76.
Jaramillo-Vogel, D., Strasser, A., Frijia, G., Spezzaferri, S., 2013. Neritic isotope and sedimentary records of the Eocene–Oligocene greenhouse–icehouse transition: the Calcare di Nago Formation (northern Italy) in a global context. Palaeogeography, Palaeoclimatology, Palaeoecology 369, 361–376.
Jenkyns, H.C., 1995. Carbon-isotope stratigraphy and paleoceanographic significance of the Lower Cretaceous shallow-water carbonates of Resolution Guyot, Mid-Pacific Mountains. Proceedings of the Ocean Drilling Program: Scientific Results 143, 99–104.
Katz, M.E., Miller, K.G., Wright, J.D., Wade, B.S., Browning, J.V., Cramer, B.S., Rosenthal, Y., 2008. Stepwise transition from the Eocene greenhouse to the Oligocene icehouse. Nature Geoscience 1, 329–334.
Kominz, M.A., Pekar, S.F., 2001. Oligocene eustasy from two-dimensional sequence stratigraphic backstripping. Geological Society of America Bulletin 113, 291–304.
Langer, M.R., Hottinger, L., 2000. Biogeography of selected "larger" foraminifera. Micropaleontology 46, 105–126.
Lear, C.H., Rosenthal, Y., Coxall, H.K., Wilson, P.A., 2004. Late Eocene to early Miocene ice sheet dynamics and the global carbon cycle. Paleoceanography 19, PA4015. http://dx.doi.org/10.1029/2004PA001039.
Lear, C.H., Bailey, T.R., Pearson, P.N., Coxall, H.K., Rosenthal, Y., 2008. Cooling and ice growth across the Eocene–Oligocene transition. Geology 36, 251–254.
Less, G., Özcan, E., 2008. The late Eocene evolution of nummulitid foraminifer *Spiroclypeus* in the Western Tethys. Acta Palaeontologica Polonica 53, 303–316.
Less, G., Özcan, E., Papazzoni, C.A., Stockar, R., 2008. The middle to late Eocene evolution of nummulitid foraminifer *Heterostegina* in the Western Tethys. Acta Palaeontologica Polonica 53, 317–350.
Lowrie, W., Lanci, L., 1994. Magnetostratigraphy of Eocene–Oligocene boundary sections in Italy: no evidence for short subchrons within chrons 12R and 13R. Earth and Planetary Science Letters 126, 247–258.
Luciani, V., 1989. Stratigrafia sequenziale del Terziario nella catena del Monte Baldo (Provincie di Verona e Trento). Memorie di Scienze Geologiche 41, 263–351.
Menegatti, A.P., Weissert, H., Brown, R.S., Tyson, R.V., Farrimond, P., Strasser, A., Caron, M., 1998. High-resolution $\delta^{13}C$ stratigraphy through the early Aptian "Livello Selli" of the Alpine Tethys. Paleoceanography 13, 530–545.
Meulenkamp, J.E., Sissingh, W., 2003. Tertiary palaeogeography and tectonostratigraphic evolution of the northern and southern Peri-Tethys platforms and the intermediate domains of the African–Eurasian convergent plate boundary zone. Palaeogeography, Palaeoclimatology, Palaeoecology 196, 209–228.
Miller, K.G., Tucholke, B.E., 1983. Development of Cenozoic abyssal circulation south of the Greenland–Scotland Ridge. In: Bott, M.H.P. (Ed.), Structure and Development of the Greenland–Scotland Ridge. Plenum Press, New York, New York, pp. 549–589.
Miller, K.G., Browning, J.V., Aubry, M.-P., Wade, B.S., Katz, M.E., Kulpecz, A.A., Wright, J.D., 2008. Eocene–Oligocene global climate and sea-level changes: St. Stephens Quarry, Alabama. Geological Society of America Bulletin 120, 34–53.
Miller, K.G., Wright, J.D., Katz, M.E., Wade, B.S., Browning, J.V., Cramer, B.S., Rosenthal, Y., 2009. Climate threshold at the Eocene–Oligocene transition: Antarctic ice sheet influence on ocean circulation. In: Koeberl, C., Montanari, A. (Eds.), Late Eocene Earth: Hothouse Icehouse, and Impacts. Geological Society of America Special Papers 452, pp. 169–178.
Moisette, P., 2000. Changes in bryozoan assemblages and bathymetric variations. Examples from the Messinian of northwest Algeria. Palaeogeography, Palaeoclimatology, Palaeoecology 155, 305–326.
Montanari, A., Sandroni, P., Clymer, A., Collins, G., Coccioni, R., Lanci, L., Lowrie, W., 1994. The MASSICORE: preliminary report on a core drilled across the Eocene–Oligocene boundary in the type locality of Massignano (Italy). Bulletin of Liaison and Information,International Geological. Correlation Project 196, 13–16.
Mort, H.P., Adatte, T., Föllmi, K.B., Keller, G., Steinmann, P., Matera, V., Berner, Z., Stüben, D., 2007. Phosphorus and the roles of productivity and nutrient recycling during oceanic anoxic event 2. Geology 35, 483–486.
Murray, J.W., 1973. Distribution and Ecology of Living Benthic Foraminiferids. Heinemann Educational, London (274 pp.).
Mutti, M., Hallock, P., 2003. Carbonate systems along nutrient and temperature gradients: some sedimentological and geochemical constraints. International Journal of Earth Sciences 92, 465–475.
Mutti, M., John, C.M., Knoerich, A.C., 2006. Chemostratigraphy in Miocene heterozoan carbonate settings: applications, limitations and perspectives. In: Pedley, H.M., Carannante, G. (Eds.), Cool-Water Carbonates: Depositional Systems and Palaeoenvironmental Controls. Geological Society, London, Special Publications 255, pp. 307–322.
Nebelsick, J.H., Rasser, M.W., Bassi, D., 2005. Facies dynamics in Eocene to Oligocene circumalpine carbonates. Facies 51, 197–217.
Nelson, C.S., Keane, S.L., Head, P.S., 1988a. Non-tropical carbonate deposits on the modern New Zeland shelf. Sedimentary Geology 60, 71–94.
Nelson, C.S., Hyden, F.M., Keane, S.L., Leask, W.L., Gordon, D.P., 1988b. Application of bryozoan zoarial growth-form studies in facies analysis of non-tropical carbonate deposits in New Zealand. Sedimentary Geology 60, 301–322.
Nocchi, M., Parisi, G., Monaco, P., Monechi, S., Madile, M., 1988. Eocene and Early Oligocene micropaleontology and paleoenvironments in SE Umbria, Italy. Palaeogeography, Palaeoclimatology, Palaeoecology 67, 181–244.
Parente, M., Frijia, G., Di Lucia, M., 2007. Carbon-isotope stratigraphy of Cenomanian–Turonian platform carbonates from the southern Apennines (Italy): a chemostratigraphic approach to the problem of correlation between shallow-water and deep-water successions. Journal of the Geological Society 164, 609–620.
Pedley, M., Carannante, G., 2006. Cool-water carbonate ramps: a review. In: Pedley, M.H., Carannante, G. (Eds.), Cool-water Carbonates: Depositional Systems and Palaeoenvironmental Controls. Geological Society, London, Special Publications 255, pp. 1–9.
Plancq, J., Mattioli, E., Pittet, B., Simon, L., Grossi, V., 2014. Productivity and sea-surface temperature changes recorded during the Late Eocene–Early Oligocene at DSDP Site 511 (South Atlantic). Palaeogeography, Palaeoclimatology, Palaeoecology 407, 34–44.
Pomar, L., 2001. Ecological control of sedimentary accommodation: evolution from a carbonate ramp to rimmed shelf, Upper Miocene, Balearic Islands. Palaeogeography, Palaeoclimatology, Palaeoecology 175, 249–272.
Premoli Silva, I., Jenkins, D.G., 1993. Decision on the Eocene–Oligocene boundary stratotype. Episodes 16, 379–382.
Pusz, A.E., Thunell, R.C., Miller, K.G., 2011. Deep water temperature, carbonate ion, and ice volume changes across the Eocene–Oligocene climate transition. Paleoceanography 26, PA2205. http://dx.doi.org/10.1029/2010PA001950.
Reid, C.M., James, N.P., Bone, Y., 2011. Carbonate sediments in a cool-water macroalgal environment, Kaikoura, New Zeland. Sedimentology 58, 1935–1952.

Romero, J., Caus, E., Rosell, J., 2002. A model for the palaeoenvironmental distribution of larger foraminifera based on late Middle Eocene deposits on the margin of the South Pyrenean basin (NE Spain). Palaeogeography, Palaeoclimatology, Palaeoecology 179, 43–56.
Salamy, K.A., Zachos, J.C., 1999. Latest Eocene–Early Oligocene climate change and Southern Ocean fertility: inferences from sediment accumulation and stable isotope data. Palaeogeography, Palaeoclimatology, Palaeoecology 145, 61–77.
Serra-Kiel, J., Hottinger, L., Caus, E., Drobne, K., Ferrandez, C., Jauhri, A.K., Less, G., Pavlovec, R., Pignatti, J., Samso, J.M., Schaub, H., Sirel, E., Strougo, A., Tambareau, Y., Tosquella, J., Zakrevskaya, E., 1998. Larger foraminiferal biostratigraphy of the Tethyan Paleocene and Eocene. Bulletin de la Societe Geologique de France 169, 281–299.
Setiawan, J.R., 1983. Foraminifera and microfacies of the type Priabonian. Utrecht Micropaleontological Bulletins 29 (161 pp.).
Shepherd, S., Edgar, G.J., 2014. Ecology of Australian Temperate Reefs: The Unique South. CSIRO Publishing (520 pp.).
Stoll, H.M., Schrag, D.P., 2000. High-resolution stable isotope records from the Upper Cretaceous rocks of Italy and Spain: glacial episodes in a greenhouse planet? Geological Society of America Bulletin 112, 308–319.
Teichert, S., Woelkerling, W., Rüggeberg, A., Wisshak, M., Piepenburg, D., Meyerhöfer, M., Form, A., Büdenbender, J., Freiwald, A., 2012. Rhodolith beds (Corallinales, Rhodophyta) and their physical and biological environment at 80°31′N in Nordkappbukta (Nordaustlandet, Svalbard Archipelago, Norway). Phycologia 51, 371–390.
Thomas, D.J., Lyle, M., Moore, T.C., Rea, D.K., 2008. Paleogene deepwater mass composition of the tropical Pacific and implications for thermohaline circulation in a greenhouse world. Geochemistry, Geophysics, Geosystems 9, Q02002. http://dx.doi.org/10.1029/2007GC001748.
Trevisani, E., 1997. Il margine settentrionale del Lessini Shelf: Evoluzione paleogeografica e dinamica deposizionale del paleogene della Valsugana (Trentino Sud-Orientale). Atti Ticinensi di Scienze della Terra 5, 115–127.
Ungaro, S., 1978. L'Oligocene dei Colli Berici. Rivista Italiana di Paleontologia 84, 199–278.
Vahrenkamp, V.C., 1996. Carbon isotope stratigraphy of the Upper Kharaib and Shuaiba Formations: implications for the Early Cretaceous evolution of the Arabian Gulf region. Bulletin of the American Association of Petroleum Geologists 80, 647–662.
Van de Schootbrugge, B., Kuhn, O., Adatte, T., Steinmann, P., Föllmi, K., 2003. Decoupling of P- and C_{org}-burial following Early Cretaceous (Valanginian–Hauterivian) platform drowning along the NW Tethyan margin. Palaeogeography, Palaeoclimatology, Palaeoecology 199, 315–331.
Villa, G., Fioroni, C., Persico, D., Roberts, A.P., Florindo, F., 2014. Middle Eocene to Late Oligocene Antarctic glaciation/deglaciation and Southern Ocean productivity. Paleoceanography 29. http://dx.doi.org/10.1002/2013PA002518.
Wade, B.S., Pearson, P.N., 2008. Planktonic foraminiferal turnover, diversity fluctuations and geochemical signals across the Eocene/Oligocene boundary in Tanzania. Marine Micropaleontology 68, 244–255.
Wade, B.S., Houben, A.J.P., Quaijtaal, W., Schouten, S., Rosenthal, Y., Miller, K.G., Katz, M.E., Wright, J.D., Brinkhuis, H., 2012. Multiproxy record of abrupt sea-surface cooling across the Eocene–Oligocene transition in the Gulf of Mexico. Geology 40, 159–162.
Westphal, H., Halfar, J., Freiwald, A., 2010. Heterozoan carbonates in subtropical to tropical settings in the present and past. International Journal of Earth Sciences 99 (Suppl. 1), S153–S169.
Wilson, M.E.J., Vecsei, A., 2005. The apparent paradox of abundant foramol facies in low latitudes: their environmental significance and effect on platform development. Earth-Science Reviews 69, 133–168.
Wright, J.D., Miller, K.G., 1993. Southern Ocean influences on late Eocene to Miocene deepwater circulation. In: Kennett, J.P., Warnke, D.A. (Eds.), The Antarctic Paleoenvironment: A Perspective on Global ChangeAntarct. Res. Ser. 60. American Geophysical Union, Washington, pp. 1–25.
Wright, C.A., Murray, J.W., 1972. Comparisons of modern and Paleogene foraminiferid distributions and their environmental implications. Mémoires du Bureau de Recherches Géologiques et Minières 79, 87–96.
Zachos, J.C., Quinn, T.M., Salamy, K.A., 1996. High-resolution (104 years) deep-sea foraminiferal stable isotope records of the Eocene–Oligocene climate transition. Paleoceanography 11, 251–266.
Zágoršek, K., 1992. Priabonian (Late Eocene) Cyclostomata Bryozoa from the Western Carpathians (Czechoslovakia). Geologica Carpathica 43, 235–247.
Zágoršek, K., 1993. Changes in bryozoan community in the Upper Eocene sequence of Mátyáshegy (Hungary). Oeslenytáni Viták (Discussiones Paleontologicae) 39, 91–96.
Zágoršek, K., 1994. Late Eocene (Priabonian) Cheilostomata Bryozoa from Liptov Basin Western Carpathians (Slovakia). Neues Jahrbuch für Geologie und Paläontologie (Abhandlungen) 193, 361–382.
Zágoršek, K., 1996. Paleoecology of the Eocene bryozoan marl in the Alpine–Carpathian region. In: Gordon, D.P., Smith, A.M., Grant-Mackie, J.A. (Eds.), Bryozoans in Space and Time. National Institute of Water & Atmospheric Research (413–422 pp.).
Zágoršek, K., 2003. Contribution to the knowledge of some cyclostomatous Bryozoa from the Eocene of Molasse Zone (Salzburg, Austria). Neues Jahrbuch fur Geologie und Paleontologie 2003 (7), 439–448.
Zágoršek, K., Darga, R., 2004. Eocene Bryozoa from the Eisenrichterstein beds, Hallthurm, Bavaria. Zitteliana A 44, 17–40.
Zágoršek, K., Kázmér, M., 1999. Late Eocene bryozoan faunas in the Alpine–Carpathian region — a comparison. Acta Paleontologica Romaniae 2, 493–504.